

Springer Series in Optical Sciences

Editorial Board: A. L. Schawlow K. Shimoda A. E. Siegman T. Tamir

Managing Editor: H. K. V. Lotsch

- 42 **Principles of Phase Conjugation**
By B. Ya. Zel'dovich, N. F. Filipetsky,
and V. V. Shkunov
- 43 **X-Ray Microscopy**
Editors: G. Schmahl and D. Rudolph
- 44 **Introduction to Laser Physics**
By K. Shimoda 2nd Edition
- 45 **Scanning Electron Microscopy**
Physics of Image Formation and Microanalysis
By L. Reimer
- 46 **Holography and Deformation Analysis**
By W. Schumann, J.-P. Zürcher, and D. Cuche
- 47 **Tunable Solid State Lasers**
Editors: P. Hammerling, A. B. Budgor,
and A. Pinto
- 48 **Integrated Optics**
Editors: H. P. Nolting and R. Ulrich
- 49 **Laser Spectroscopy VII**
Editors: T. W. Hänsch and Y. R. Shen
- 50 **Laser-Induced Dynamic Gratings**
By H. J. Eichler, P. Günter, and D. W. Pohl
- 51 **Tunable Solid State Lasers for Remote Sensing**
Editors: R. L. Byer, E. K. Gustafson,
and R. Trebino
- 52 **Tunable Solid-State Lasers II**
Editors: A. B. Budgor, L. Esterowitz,
and L. G. DeShazer
- 53 **The CO₂ Laser** By W. J. Witteman
- 54 **Lasers, Spectroscopy and New Ideas**
A Tribute to Arthur L. Schawlow
Editors: W. M. Yen and M. D. Levenson
- 55 **Laser Spectroscopy VIII**
Editors: W. Persson and S. Svanberg
- 56 **X-Ray Microscopy II**
Editors: D. Sayre, M. Howells, J. Kirz,
and H. Rarback
- 57 **Single-Mode Fibers Fundamentals**
By E.-G. Neumann
- 58 **Photoacoustic and Photothermal Phenomena**
Editors: P. Hess and J. Petzi
- 59 **Photorefractive Crystals in Coherent Optical Systems**
By M. P. Petrov, S. I. Stepanov,
and A. V. Khomenko
- 60 **Holographic Interferometry in Experimental Mechanics**
By Yu. I. Ostrovsky, V. P. Shchepinov,
and V. V. Yakovlev
- 61 **Millimetre and Submillimetre Wavelength Lasers** A Handbook of cw Measurements
By N. G. Douglas
- 62 **Photoacoustic and Photothermal Phenomena II**
Editors: J. C. Murphy, J. W. MacLachlan Spicer,
L. C. Aamodt, and B. S. H. Royce
- 63 **Electron Energy Loss Spectrometers**
The Technology of High Performance
By H. Ibach
- 64 **Handbook of Nonlinear Optical Crystals**
By V. G. Dmitriev, G. G. Gurzadyan,
and D. N. Nikogosyan
- 65 **High-Power Dye Lasers**
Editor: F. J. Duarte
- 66 **Silver Halide Recording Materials for Holography and Their Processing**
By H. I. Bjelkhagen
- 67 **X-Ray Microscopy III**
Editors: A. G. Michette, G. R. Morrison,
and C. J. Buckley
- 68 **Optical Phase Conjugation**
Editors: M. C. Gower and D. Proch
- 69 **Photoacoustic and Photothermal Phenomena III**
Editor: D. Bićanić

D. Bićanić (Ed.)

Photoacoustic and Photothermal Phenomena III

Proceedings of the 7th International
Topical Meeting, Doorwerth, The Netherlands,
August 26–30, 1991

With 501 Figures

Springer-Verlag
Berlin Heidelberg New York
London Paris Tokyo
Hong Kong Barcelona
Budapest

Photoacoustic and Photothermal Investigations of Thin Films

E. Matthias, H. Grönbeck, E. Hunger, J. Jauregui, H. Pietsch, M. Reichling, S. Petzoldt, E. Welsch¹, and Z.L. Wu²

Fachbereich Physik, Freie Universität Berlin,
Arnimallee 14, W-1000 Berlin 33, Fed. Rep. of Germany
On leave from ¹Institute of Optics and Quantum Electronics,
Friedrich-Schiller-University Jena, Max-Wien Platz 1,
O-6900 Jena, Fed. Rep. of Germany

²Shanghai Institute of Optics and Fine Mechanics,
Academia Sinica, P.O. Box 800-211, Shanghai, P.R. of China

Abstract. Three different techniques - mirage effect, photothermal displacement, and thermorefectance - have been installed for investigating ablation thresholds and thermal properties of thin films. By monitoring the shock wave signal the mirage effect was used to measure ablation thresholds of optical coatings. For multilayer systems of type polymer-metal SiO_2 changes in the shock wave signal allowed to distinguish between the ablation of different layers. The photothermal displacement method was applied to measure periodicity and decay of transient thermal gratings on surfaces of thin films. This technique yields information about lateral and vertical heat diffusion and is, therefore, sensitive to anisotropic heat transport in thin films. The potential of this technique for precise measurements of thermal diffusivities is illustrated for thin films of gold and amorphous diamond.

1. Introduction

During the past decade thermal properties of thin films have received increased attention [1,2]. They are inherently connected with the quality of thin films and are, therefore, most appropriate for their characterization. Precise measurements of thermal diffusivities provide information about finite size effects, structural anisotropies, interface absorption, defect and impurity absorption, and incubation effects. Also, it has been suggested by several workers in the field [3,4] that optical damage thresholds are strongly correlated to thermal properties of thin films, which means that these also play an important role for laser processing of thin films. Hence, the interest in thermal data ranges from optical, protective, and polymer coatings to semiconducting and metallic films as well as to high- T_c superconducting films.

These prospects led us to start an activity where several techniques like mirage effect, photothermal displacement and thermorefectance are employed to yield complementary information about the same or similar film material. We also find it important to work both in the time and frequency

domain in order to have the possibility for cross-checking the results. One ultimate goal of this project is to quantitatively correlate ablation thresholds to thermal properties of thin films. This contribution summarizes the present status of the work on thin films in our laboratory by presenting informative examples for each technique.

2. Damage thresholds measured by the mirage effect

The mirage effect caused by the transient change of refractive index [5-7] measures both acoustic and thermal waves emerging from a surface when irradiating it with laser pulses of sufficiently large fluence. They can be distinguished by their range as well as by their speed. This technique is particularly well suited for studying ablation thresholds and the development of laser-induced plasmas, in which case the thermal wave is substituted by the plasma wave. A typical signal obtained from a Kapton foil with a fluence above the ablation threshold is displayed in the lower part of Fig. 1. It shows a fast signal which we attribute to the refractive index gradient caused by the shock or blast wave. The huge later signal reflects the slowly expanding plasma. Deflection signals from PMMA recorded at 20 times higher fluences are very similar in shape, hence, we consider the one in Fig. 1 as being generally representative for different types of material. In fact, it very closely resembles the pictures taken by an ultrafast imaging technique at above threshold fluences with polyimide [8] and PMMA [9]. Notice, however, that the "clean" signal in Fig. 1 can, for certain materials, be badly distorted by probe laser scattering from large size fragments leaving the surface.

When applying the mirage technique to the investigation of ablation thresholds both the shock and plasma signals in Fig. 1 yield identical results, for example for polyimide. Because of its superior reproducibility, however, we prefer to use the fast shock wave signal for measuring optical damage thresholds. An example is shown in Fig. 2, where the deflection signal is plotted as a function of fluence for both pure

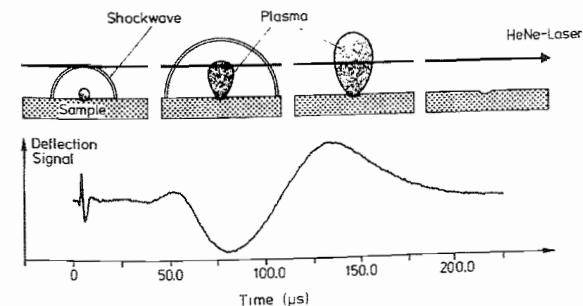


Fig. 1: Mirage effect signal from polyimide at a fluence of 0.12 J/cm^2 (lower part). The upper part sketches the origin of the two different refractive index changes.

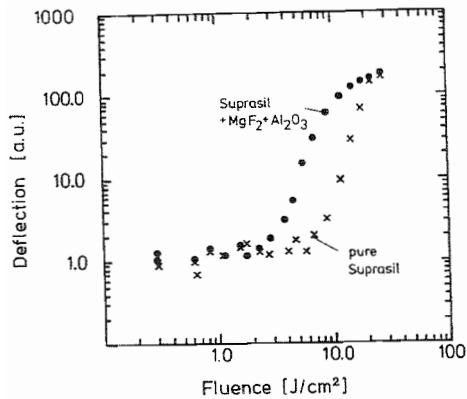


Fig. 2: Reduction of optical damage threshold by an optical coating on suprasil, measured by the shock wave mirage deflection signal at a pump laser wavelength of 248 nm [10].

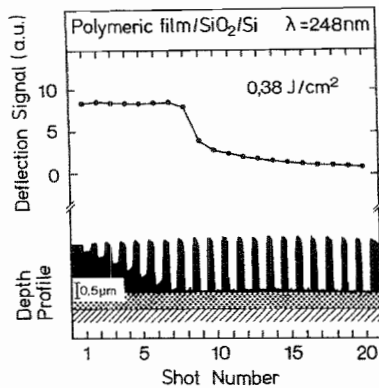


Fig. 3: Change of the shock wave mirage deflection signal at the transition from a photoresist film to a SiO₂ layer [12]. The lower part of the figure indicates the thickness scale and shows the depth profile of the photoresist layer.

suprasil and suprasil antireflex-coated with MgF₂ and Al₂O₃. Obviously, the coating causes a substantial lowering of the damage threshold. More detailed studies show that the reduction is due to the Al₂O₃-layer, including its interface while the MgF₂ coating alone causes no decrease. The underlying mechanism for this behavior remains to be investigated and calls for a measurement of the thermal diffusivities of these coatings.

For a given laser fluence the amplitudes of both signals in Fig. 1 depend on the absorbance of the material. Consequently the shock wave signal can also be utilized to distinguish between the ablation of layers of different materials [11]. This is illustrated in Fig. 3, where we can see that about 8 laser shots of 0.38 J/cm² at 248 nm are needed to remove a 1.5 μm thick film of photoresist. The deflection signal undergoes a step-like change when the laser light reaches the SiO₂ layer which has a much higher ablation

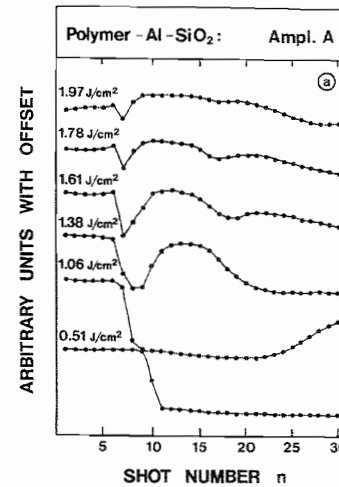


Fig. 4: Shock wave mirage deflection signals for a multilayer system [12] exposed to various fluences at 248 nm as a function of laser shots. The first step indicates penetration of the polymer layer, the following increase and maximum reflects ablation of the Al layer.

threshold and consequently no shock wave is generated. The small and decreasing signal above 8 shots is due to cleaning of residual photoresist and etching of the walls. Measurements of the etch depth profile were carried out to verify this interpretation and are shown in the lower part of Fig. 3.

This technique still works for multilayer systems provided the damage thresholds of the materials involved differ significantly. To demonstrate this point the film sequence polymer-metal-SiO₂ was irradiated with 248 nm light at various fluences [13]. The result for a sample with an Al-layer is shown in Fig. 4. Again, in the fluence range used the ablation of the photoresist starts at the first shot. The fluence of 0.51 J/cm² is too low to damage the Al-film with 30 shots. For 1.06 J/cm² we notice an increase of the deflection signal after about 25 shots, indicating the onset of metal ablation. At 1.38 J/cm² this onset is shifted to 10 shots, and starts still earlier at higher fluences. One can even notice an indication of SiO₂ breakup around 20 shots at 1.61 J/cm². Clearly, the contrast in the deflection signal between different layers is lost at higher fluences (> 1.7 J/cm²), but within a certain fluence range it is possible to monitor the ablation of individual layers in multilayer systems [14].

3. Thermal diffusivities measured by displacement detection of transient thermal gratings

The pulsed photothermal displacement technique [15] is in principle an ideal tool for measuring the thermal diffusivity κ of thin films since the thermal diffusion length, $L_{th} = 2(\kappa\tau_0)^{1/2}$, is of the order of micrometer or less for a laser pulse length, τ_0 , of nanoseconds or shorter. To our knowledge, however, only few attempts have been made to apply this

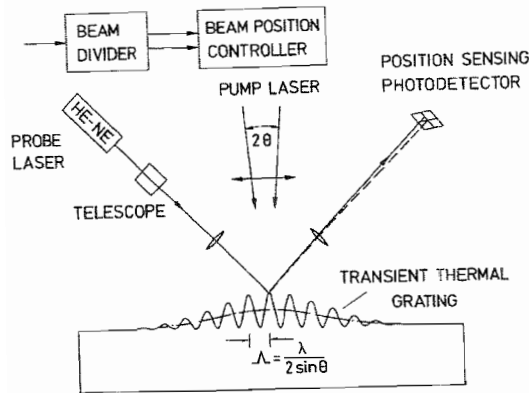


Fig. 5: Principle experimental scheme for photothermal displacement measurements on transient thermal gratings.

technique to thin films [16]. The reason may be that the intensities required for a good signal-to-noise ratio often come close to the damage thresholds of thin films. In the following we want to demonstrate that this technique can be considerably refined by combining it with the excitation of transient thermal gratings (TTG's) [17] on the film surface.

The use of TTG's instead of a circular beam spot brings several advantages: (1) It defines a direction in the surface plane and thereby becomes sensitive to anisotropic lateral heat diffusion. (2) Under certain conditions [18] theory predicts the following simple relation between the effective decay rate τ_{eff}^{-1} and the periodicity Λ of the grating:

$$\tau_{\text{eff}}^{-1} = \left(\frac{2}{a^2} + \frac{4\pi^2}{\Lambda^2} \right) \kappa + \tau_z^{-1} \quad (1)$$

where a is the extension of the grating perpendicular to its periodicity, and τ_z^{-1} takes into account the vertical heat diffusion. Hence a measurement of the exponential decay time, the periodicity, and the width of the grating leads to values for the thermal diffusivity and the vertical diffusion rate. (3) As long as the theoretical approximations are valid this technique leads to a good accuracy for the thermal diffusivity since τ_{eff} , Λ , and a can be measured rather precisely. Notice, however, that strictly speaking the technique determines the diffusivity constant for heat transport in the plane of the film.

The experimental set-up for probing the surface displacement of TTG's by reflecting a HeNe-laser beam is sketched in Fig. 5. The change in the reflection angle is recorded by a quadrant diode. The HeNe-laser is always focussed to the same surface spot (beam diameter about 50 μm) while the interference pattern generated by the two pump beams (wavelength 543 nm, pulsewidth 4 ns) is moved across this

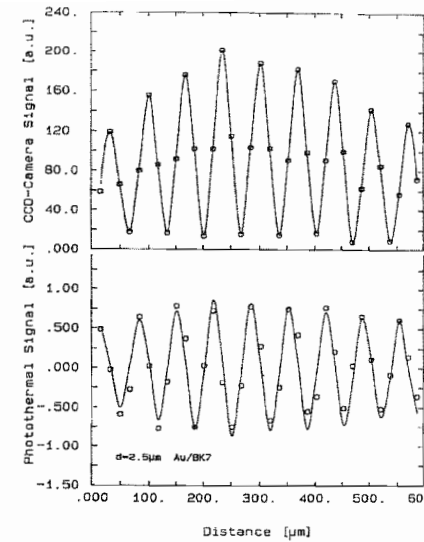


Fig. 6: TTG on a 2.5 μm gold film (lower part) generated by the interference pattern shown in the upper part of the figure. The latter was recorded by a CCD camera. The solid line in the upper part is a fit to the data points yielding $\Lambda = 67.3 \mu\text{m}$. Its derivative is the solid line in the lower part.

spot. Before a grating is measured the interference pattern is recorded by a CCD-camera to control its general shape and to measure its width a . Scans of the CCD-camera recording and of the corresponding TTG on the surface of a 2.5 μm gold film on BK7 glass are compared in Fig. 6. The phase shift between both patterns is $\pi/2$ since the displacement technique measures the derivative of the grating. We notice the excellent agreement between the two different sets of data. It also is obvious that a fit to the grating in the lower part of Fig. 6 will lead to an accurate value of the periodicity Λ .

The second important quantity needed for Eq.(1) is the effective decay rate. In Fig. 7 we show typical decays of TTG's on gold films of different thicknesses on a BK7 glass substrate [19]. Notice that in each case the decay is well described by a single exponential function indicated by solid lines. The striking difference between the decay constants for films of 100 nm and 2.5 μm reflects the influence of finite size effects, the increase of structural defects with decreasing thickness [20], and an increase of vertical heat flow with increasing thickness [19]. The latter, however, is not as important as one might expect, since the straight lines in Fig. 8, fitted to the data according to Eq.(1), intersect the ordinate at roughly the same value. The strong thickness dependence of the slopes corresponds to the different decay times in Fig. 7, and shows the drastic reduction of the thermal diffusivity with film thickness.

The fact that the straight lines in Fig. 8 fit the data well gives faith in the theoretical model and the validity of Eq.(1). However, as discussed in Ref. [19] our results for the thermal diffusivities are significantly smaller compared to the values obtained by other techniques. For example, photothermal reflectance measurements with MHz modulated

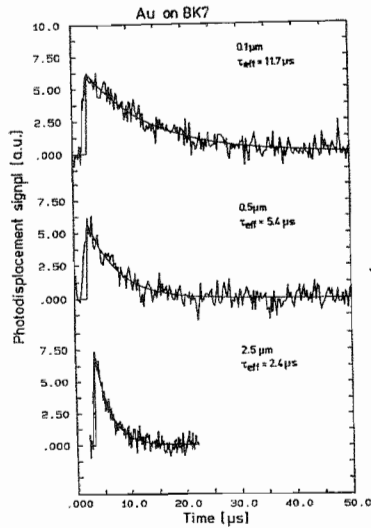


Fig. 7: Decay of TTG's on gold films of different thicknesses. Solid lines are fits to the data resulting in the decay constants shown.

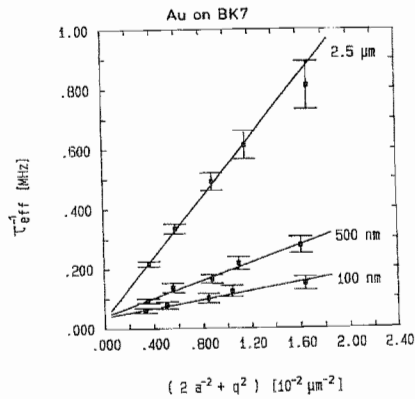


Fig. 8. Averaged effective decay rates for gold films of different thicknesses plotted according to Eq.(1). The slope of each line yields the thermal diffusivity. The results are in cm^2s^{-1} : 0.07, 0.15, 0.50 for the thicknesses 100, 500, and 2500 nm, respectively.

Ar^+ -laser light carried out at our laboratory [21] reproduced for the 2.5 μm film the bulk value of $1.25 \text{ cm}^2\text{s}^{-1}$, in contrast to $0.50 \text{ cm}^2\text{s}^{-1}$ obtained from the fit in Fig. 8. For a 1 μm film the thermoreflectance measurement yields $1.0 \text{ cm}^2\text{s}^{-1}$ while the TTG displacement technique gives $0.4 \text{ cm}^2\text{s}^{-1}$. The latter technique does not even replicate the bulk value when applied to a 210 μm gold plate, instead we obtain the 25 % lower value of $0.94 \text{ cm}^2\text{s}^{-1}$. The deviations are systematically toward lower values and much larger than the experimental uncertainty of about 5 %. We propose that these are caused by surface texture, island structure and other defects [22], and that they reflect the sensitivity of the TTG displacement technique to lateral heat diffusion. Further evidence for this is obtained by studying the influence of surface morphology on the thermal diffusivity. Fig. 9a shows a microscopy picture of the gold plate surface for which the measurement resulted in a 25 % reduced value of κ . The random texture apparently diminishes the lateral heat conduction. Such is not the case for the polished Ni surface (Fig. 9b) for which we measure $\kappa(\text{Ni}) = 0.23 \pm 0.01 \text{ cm}^2\text{s}^{-1}$, in perfect agreement with the literature bulk value of $0.22 \text{ cm}^2\text{s}^{-1}$ [18]. The surface of a Ni-foil shown in Fig. 9c provides an example for a strongly anisotropic lateral heat diffusion. If we align the wave vector, $q = 2\pi/\Lambda$, of the TTG parallel to the grooves we find $\kappa_{\parallel} = 0.19 \pm 0.03 \text{ cm}^2\text{s}^{-1}$, while the thermal diffusivity perpen-

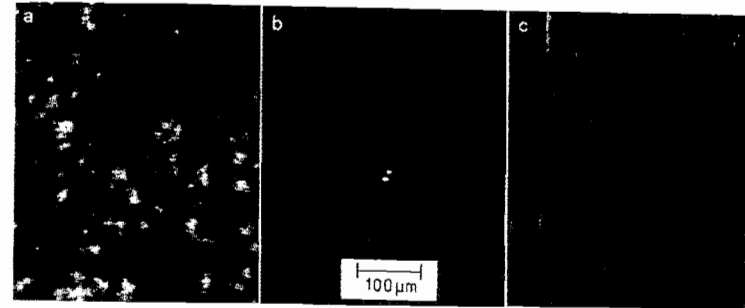


Fig. 9: Dependence of thermal diffusivities on surface morphology. (a) surface structure of 210 μm Au-plate (purity 99.8. %); (b) polished surface of Ni (99.98 %); (c) surface structure of 20 μm Ni-foil (99.98 %).

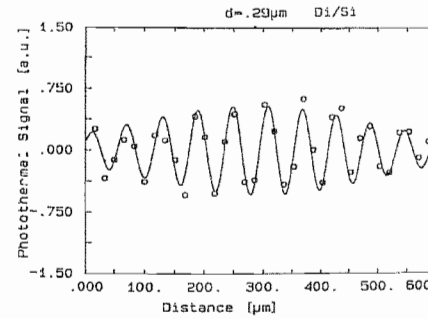


Fig. 10: TTG pattern on a 0.29 μm amorphous diamond film on silicon [24]. The solid line represents a fit to the data, yielding $\Lambda = 59 \mu\text{m}$.

dicular to the grooves is reduced to $\kappa_{\perp} = 0.05 \pm 0.02 \text{ cm}^2\text{s}^{-1}$. These examples confirm that the TTG displacement technique measures predominantly the lateral heat flow in a rather shallow layer defined by the grating amplitude, and that q^2 is the leading term in Eq.(1). Hence this technique is ideally suited for studying the structural quality of thin films.

Due to their small optical absorption depth and the poor thermal conductivity of the substrate, metal films on glass represent a favorable case for the TTG displacement technique. The question is whether Eq.(1) will still be applicable when the optical absorption depth is comparable or even larger than the film thickness. To a first approximation one expects that the technique is useful as long as a TTG can be detected. For very thin films, however, it must be checked that the TTG is not formed at the substrate surface. A most interesting case close to the limit of validity are hydrogen-free "amorphous diamond" films with a typical optical absorption length of 0.2 μm [23]. A well developed TTG on a 0.29 μm thick film of this kind is shown in Fig. 10, and a

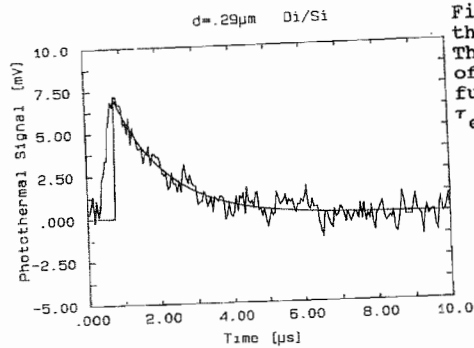


Fig. 11: Typical decay of the TTG shown in Fig. 10. The solid line is the fit of a single exponential function to the data with $\tau_{\text{eff}} = 1,45 \mu\text{s}$.

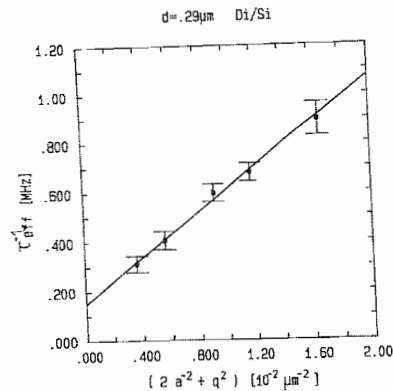


Fig. 12: Averaged effective decay rates for five different TTG's on a $0.29 \mu\text{m}$ amorphous diamond film [24] plotted according to Eq.(1). The solid line represents a fit to the data.

typical decay curve can be seen in Fig. 11. Many of those decay curves were measured and the results averaged to give the effective decay rates plotted in Fig. 12 for five different gratings in the form dictated by Eq.(1). The straight line is a fit to the data with the result $\kappa = (0.45 \pm 0.03) \text{cm}^2 \text{s}^{-1}$ and $\tau = 6.7 \mu\text{s}$. Again the data are perfectly well described by z^2 a straight line, which makes us confident that thermal diffusivities of diamond films can be measured by this technique down to thicknesses of about $0.2 \mu\text{m}$, depending on their absorption coefficient. This offers the possibility to utilize this type of measurement for a quality control of thin diamond films.

4. Conclusions

It was shown that the mirage deflection signal, caused by the shock wave emerging from the surface, is an ideal tool to measure optical damage thresholds of coatings. It can also be

successfully used to monitor the selective ablation of thin films whenever the damage thresholds of film and substrate differ. Within a certain fluence range, determined by the ablation thresholds of the materials involved, this is still true for multilayer systems. Therefore the shock wave detection has great potential for in-situ controlling laser structuring of thin films.

In order to obtain thermal diffusivities with good accuracy the displacement detection of TTG's was introduced. The power of the technique was demonstrated for gold films on glass and amorphous diamond films on Si. It was shown that the TTG displacement technique is most sensitive for lateral heat diffusion. Therefore the results may be affected by the surface texture. Since the TTG introduces a direction, this technique is well suited for studying anisotropic lateral heat transport.

This work was supported by the Deutsche Forschungsgemeinschaft, Sfb 337, and by the Bundesministerium für Forschung und Technologie, contract No. 13N5627. E.W. and Z.L.W. acknowledge fellowships from the Alexander von Humboldt-Stiftung. J.J. was supported by the Deutscher Akademischer Austauschdienst (DAAD).

References

1. P. Hess (editor): Photoacoustic, Photothermal and Photochemical Processes at Surfaces and in Thin Films, Topics in Current Physics Vol. 47, Springer Verlag Berlin-Heidelberg 1989
2. J.C. Murphy, J.W. MacLachlan Spicer, L.C. Aamodt, B.S.H. Royce (editors): Photoacoustic and Photothermal Phenomena II, Part III, Springer Ser. Opt. Sci. 62 (1990)
3. E. Welsch, H.G. Walther, D. Schäfer, R. Wolf: Thin Solid Films 152, 433 (1987)
4. J.C. Lambropoulos, M.R. Jolly, C.A. Amsden, S.E. Gilman, M.J. Sinicropi, D. Diakomihalis, S.D. Jacobs: J. Appl. Phys. 66, 4230 (1989)
5. W.B. Jackson, N.M. Amer, A.C. Boccara, D. Fournier: Appl. Opt. 20, 1333 (1981)
6. H.M. Lai, K. Young: J. Acoust. Soc. Am. 72, 2000 (1982)
7. S. Petzoldt, A.P. Elg, M. Reichling, J. Reif, E. Matthias: Appl. Phys. Lett. 53, 2005 (1988)
8. R. Srinivasan, K.G. Casey, B. Braren, M. Yeh: J. Appl. Phys. 67, 1604 (1990)
9. R. Srinivasan, B. Braren, K.G. Casey: J. Appl. Phys. 68, 1842 (1990)
10. Samples were kindly provided by Wild-Leitz AG
11. E. Hunger, S. Petzoldt, H. Pietsch, J. Reif, and E. Matthias: SPIE Vol. 1441, 283 (1990)
12. The sample was kindly provided by Dr. E. Neske, Fraunhofer Institut für physikalische Meßtechnik, Freiburg
13. E. Hunger, H. Pietsch, S. Petzoldt, E. Matthias: Appl. Surf. Sci., in print
14. E. Hunger, H. Pietsch, S. Petzoldt, E. Matthias: SPIE Vol. 1598, to be published

15. C. Karner, A. Mandel, F. Träger: *Appl. Phys.* **A38**, 19 (1985)
16. Q. Kong, J. Fischer, F. Träger: p. 179 in *Photoacoustic and Photothermal Phenomena*, editors: P. Hess, J. Pelzl, Springer Ser. Opt. Sci. **58** (1988)
17. H. Eichler, P. Günter, D.W. Pohl: *Laser-Induced Dynamic Gratings*, Springer Ser. Opt. Sci. **50** (1986)
18. J. Jauregui, E. Matthias: to be published, and contributed paper to this conference
19. J. Jauregui, Z.L. Wu, D. Schäfer, E. Matthias: contributed paper to this conference
20. P. Nath, K.L. Chopra: *Thin Solid Films* **20**, 53 (1974)
21. M. Reichling, Thesis, Freie Universität Berlin 1991
22. I.J. Hodgkinson, P.W. Wilson: *CCR Critical Reviews in Solid State and Material Sciences* **15**, 27 (1988)
23. F. Davanloo, E.M. Juengerman, D.R. Jander, T.J. Lee, C.B. Collins: *J. Appl. Phys.* **67**, 2081 (1990)
24. The sample was kindly provided by professor C.B. Collins, University of Texas at Dallas

Signal Enhancement and Noise Suppression Considerations in Photothermal Spectroscopy

A.C. Tam

IBM Research Division, Almaden Research Center,
650 Harry Road, San Jose, CA 95120-6099, USA

Abstract. This paper provides physical discussions of factors controlling sensitivity in photothermal spectroscopy, in particular, photoacoustic spectroscopy and probe-beam deflection spectroscopy. We consider the physical basis for signal generation and enhancement methods for pulsed and continuous-modulated excitations as well as the various sources of noises which become significant when the absorption approaches the part-per-million level or below. Proper signal enhancement and noise suppression are essential to make photothermal spectroscopy a sensitive tool.

1. Introduction

Photothermal (PT) spectroscopy detects certain transient thermal effects in, on, or near a sample irradiated by a modulated excitation beam. It relies on the existence of a "thermal de-excitation" branch (see Fig. 1), which occurs for most materials. As this beam is scanned in wavelength, the PT effect is correspondingly monitored either in magnitude or in shape so that an "excitation spectrum" of the sample is obtained. This technique of PT spectroscopy is in principle "zero-background," which means that if there is no optical absorption, there is no PT signal. This is in contrast to conventional "subtractive" techniques involving the measurement of transmitted or reflected beams from the sample.

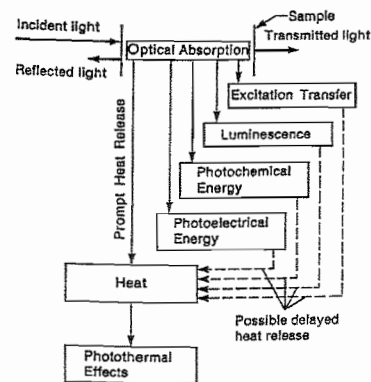


Figure 1. Schematics of optical absorption and de-excitation channels that can lead to "prompt" and "delayed" photothermal effects.